

Electronic Supporting Information for

Heterogeneous Li coordination in Solvent-in-Salt electrolytes enables high Li transference numbers

Anne Hockmann^{a,b}, Florian Ackermann^{a,c}, Diddo Diddens^{a,d}, Isidora Cekic-Laskovic^d, Monika Schönhoff^{*a}

^a Institute of Physical Chemistry, University of Münster, Corrensstraße 28/30, 48149 Münster, Germany. E-mail: schoenho@uni-muenster.de

^b International Graduate School Battery Chemistry, Characterization, Analysis, Recycling, and Application (BACCARA), University of Münster, Corrensstraße 40, 48149 Münster, Germany.

^c Current address: BASF SE, Carl-Bosch-Straße 38, 67056 Ludwigshafen/Rhein, Germany.

^d Helmholtz Institute Münster, IEK-12, Forschungszentrum Jülich GmbH, Corrensstraße 48, 48149 Münster, Germany.

Contents	Page no.
A. Electrolyte compositions and densities	1
B. Ionic conductivity and ionicity	2
C. Spin relaxation	3
D. Electrophoretic NMR: Phase shifts	3
E. Onsager coefficients	4
F. Raman spectra	4
G. Self-diffusion coefficients from PFG-NMR and MD simulations	5
H. NMR spectra	5
I. MD simulations: 1 st Coordination shell of Li ⁺	5

A. Electrolyte compositions and densities

Table S1 Details of the experimentally evaluated samples showing the molal conducting salt concentration b_{salt} , the molar conducting salt concentration c_{salt} , the measured density ρ , the mass- and volume-ratios of LiTFSI salt to solvent mixture, as well as the total oxygen-to-lithium ratio.

	$b_{\text{salt}} / (\text{mol L}^{-1})$	$c_{\text{salt}} / (\text{mol L}^{-1})$	$\rho / (\text{g cm}^3)$	$m_{\text{salt}}/m_{\text{solvent}}$	$V_{\text{salt}}/V_{\text{solvent}}$	O/Li
	1	0.90	1.12	0.30	0.22	28
	2	1.60	1.23	0.60	0.43	16
	3	2.15	1.31	0.89	0.65	12
	4	2.61	1.38	1.19	0.86	10
SiS region	5	2.98	1.43	1.49	1.08	9
	6	3.28	1.47	1.79	1.29	8
	7	3.51	1.49	2.08	1.51	7

The molal salt concentration b_{salt} is defined as the quotient of the amount of conducting salt n_{salt} and the volume of the solvent mixture V_{solvent} :

$$b_{\text{salt}} = \frac{n_{\text{salt}}}{V_{\text{solvent}}} \quad (\text{S1})$$

B. Ionic conductivity and ionicity

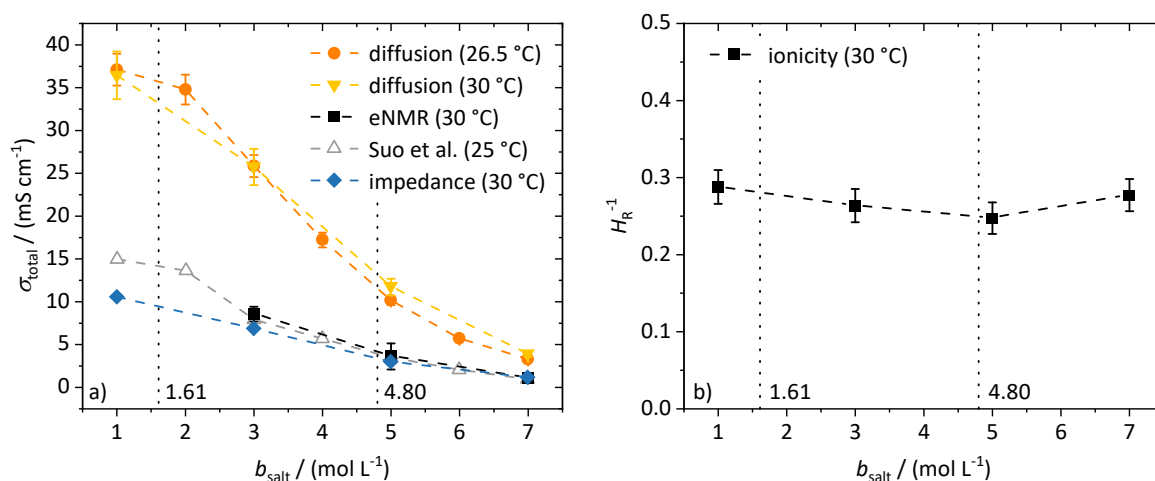


Fig. S1 a) Ionic conductivities σ_{total} determined via impedance spectroscopy, eNMR, and estimated from diffusion NMR measurements according to eq. 4 in dependency of the molal conducting salt concentration b_{salt} . The results are compared to literature values (gray) obtained by impedance spectroscopy, too.¹ b) Ionicities H_R^{-1} , obtained from diffusion NMR and impedance spectroscopy measurements (see eq. 3) plotted against the molal conducting salt concentration b_{salt} . The dashed lines in both graphs serve as guide to the eye, and the vertical dotted lines result from a model-based interpretation marking different regimes of the lithium coordination shell.

C. Spin relaxation

The measured R_1 and R_2 relaxation rates presented in Fig. S2 exhibits an increasing trend for all investigated nuclei of the different species. The increase arises mostly from the overall decrease of system dynamics. However, Fig. S2b shows that $R_1(\text{DME}) > R_1(\text{DOL})$ indicating that DME is stronger and to a higher extent coordinated and therefore less mobile leading to a higher R_1 relaxation rate compared to DOL. Therefore, these findings are in agreement with the results from the self-diffusion determination measurements. Moreover, it is shown that the relaxation rates of DME1 are higher than the rates of DME2. This is due to the fact, that the protons located at the C-atoms between the O-atoms are less flexible compared to the H-atoms of the methyl groups, which can rotate more freely. In contrast, it is found that the relaxation rates of the different H-atoms of the DOL molecule are more or less the same, since the local environment and degrees of freedom are comparable. A closer look at the relaxation rates of the ions in Fig. S2a reveals that $R_2 > R_1$ in case of the anion in the SiS region while R_1 is still equal to R_2 for Li^+ . Since $R_2 > R_1$ is obtained for longer correlation times in more viscous or solid samples, it can be suggested that the mobility of TFSI^- is in general more reduced by an increasing amount of conducting salt, while Li^+ is still quite mobile and less immobilized by ionic aggregates.

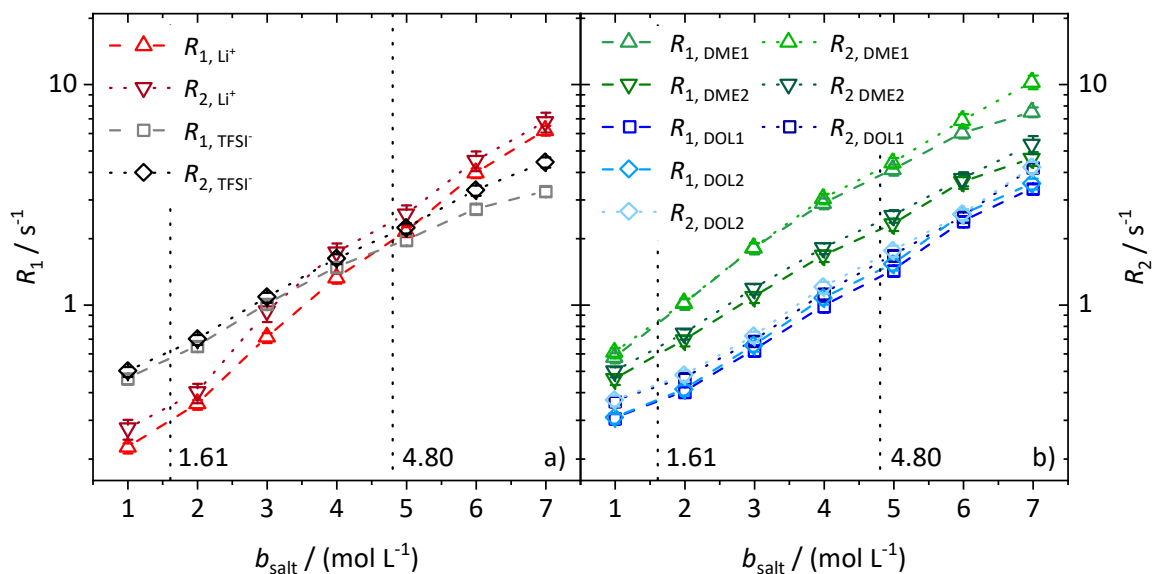


Fig. S2. R_1 (dashed lines) and R_2 (dotted lines) relaxation rates of the ions Li^+ and TFSI^- in a) and of the different protons of the solvents DME and DOL in b). The labelling of the protons is depicted in Scheme 1. The dashed and dotted lines connecting the data points in both graphs serve as guide to the eye, and the vertical dotted black lines result from a model-based interpretation marking different regimes of the lithium coordination shell.

D. Electrophoretic NMR: Phase shifts

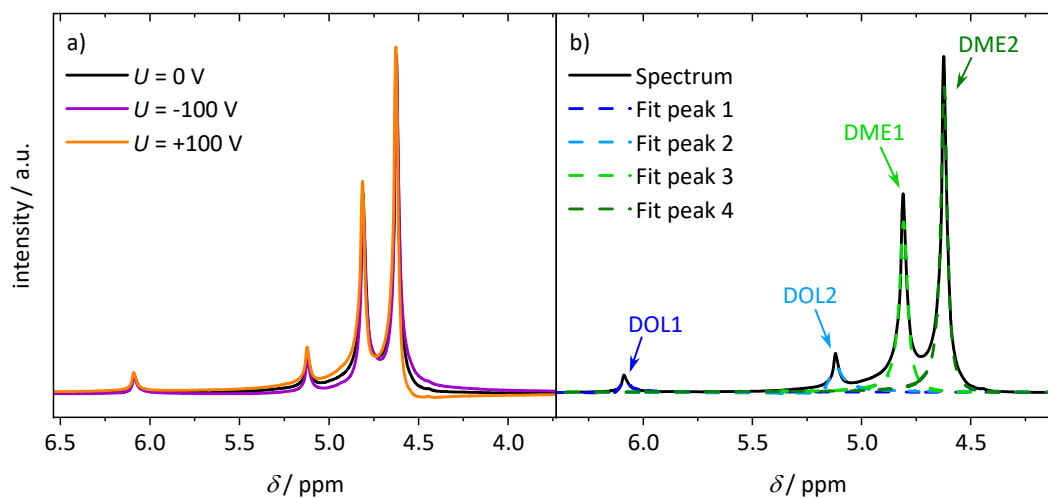


Fig. S3 ^1H eNMR spectra of 7 M LiTFSI in DME/DOL electrolyte a) at different voltage U for 0 V, -100 V, and +100 V, and b) spectrum at 0 V with deconvolution of individual ^1H resonances by Lorentzian shapes (dashed lines).

E. Onsager coefficients

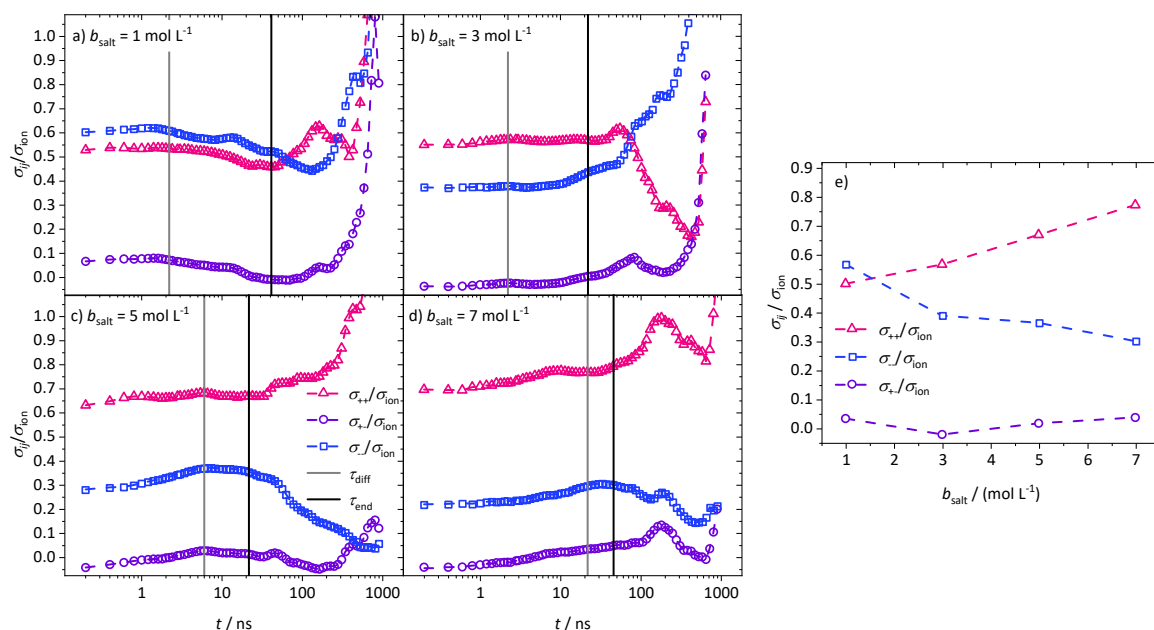


Fig. S4 a)-d): Time evolution of the Onsager coefficients σ_{ij} normalized to σ_{ion} , as calculated from MD simulations for the conducting salt concentrations 1 M, 3 M, 5 M, and 7 M, respectively. Each vertical gray line corresponds to the onset of the diffusive region as identified from the respective mean square displacements. For simulation times above the vertical black line deviations occur due to a deterioration of statistics with increasing time. Therefore, the interval between the two vertical lines was chosen to extract the actual σ_{ij}/σ_{ion} value by fitting a constant plateau to the data. These values are shown in e) in dependency on the molal salt concentration.

F. Raman spectra

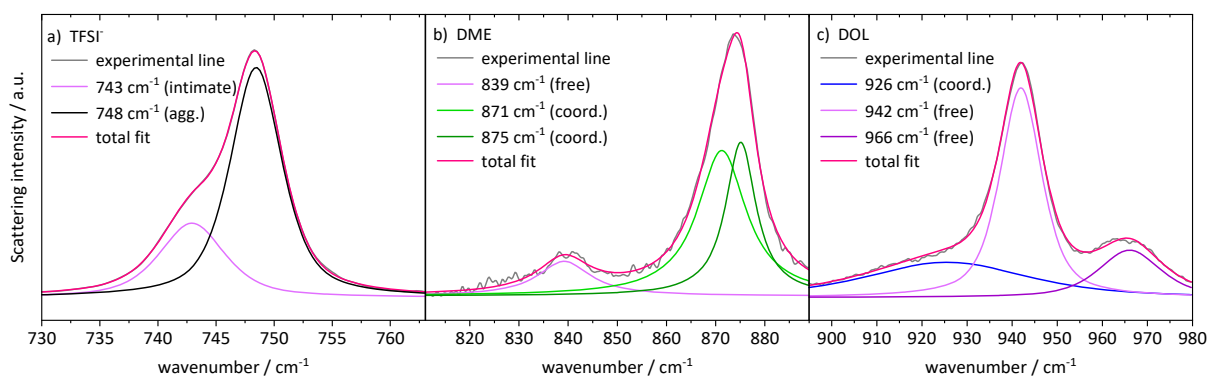


Fig. S5 Exemplary Raman spectra of the analyzed vibrational bands at a molal conducting salt concentration of 4 M in DME/DOL-based electrolyte: a) TFSI, b) DME, c) DOL.

G. Self-diffusion coefficients from PFG-NMR and MD simulations

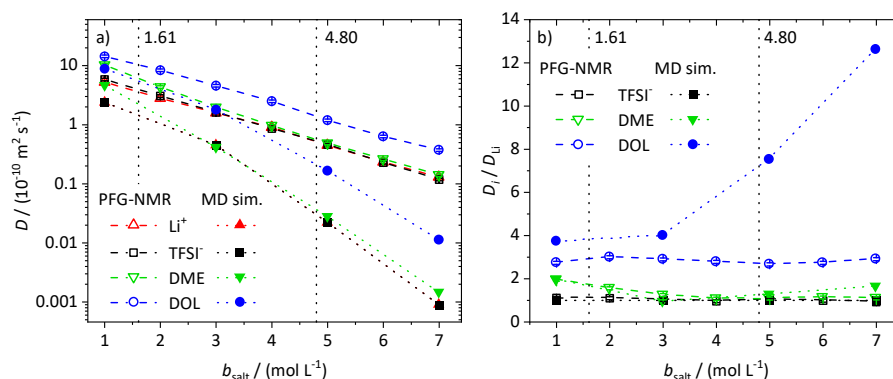


Fig. S6 a) Self-diffusion coefficients D_i of the different species obtained via PFG-NMR (open symbols) and calculated from the mean squared displacements of MD simulations (closed symbols). b) Comparison of the self-diffusion coefficient ratios D_i / D_{Li} of the different species obtained by PFG-NMR (open symbols) and MD simulations (closed symbols). The dashed and dotted lines connecting the data points in both graphs serve as guide to the eye, and the vertical dotted black lines result from a model-based interpretation marking different regimes of the lithium coordination shell.

H. NMR spectra

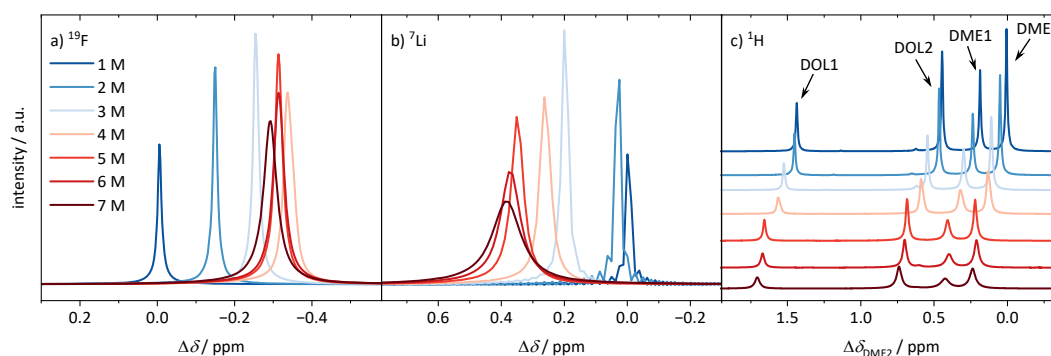


Fig. S7 Chemical shift difference $\Delta\delta$ referred to the chemical shift of the depicted species in 1 M DME/DOL-based electrolyte: a) TFSI, b) Li, c) DME2. The labelling is according to Scheme 1.

I. MD simulations: 1st Coordination shell of Li⁺

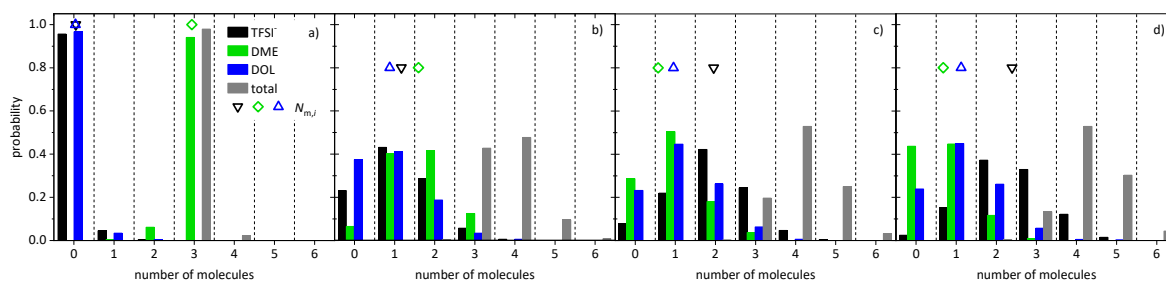


Fig. S8 Relative frequency of the number of molecules in the first coordination shell of Li⁺ and $N_{m,i}$ (average molecular coordination number given as symbol at the top of each graph) of the anion (black), DME (green), and DOL (blue), as well as the total number of molecules (gray), for the conducting salt concentrations: a) 1 M, b) 3 M, c) 5 M, d) 7 M.

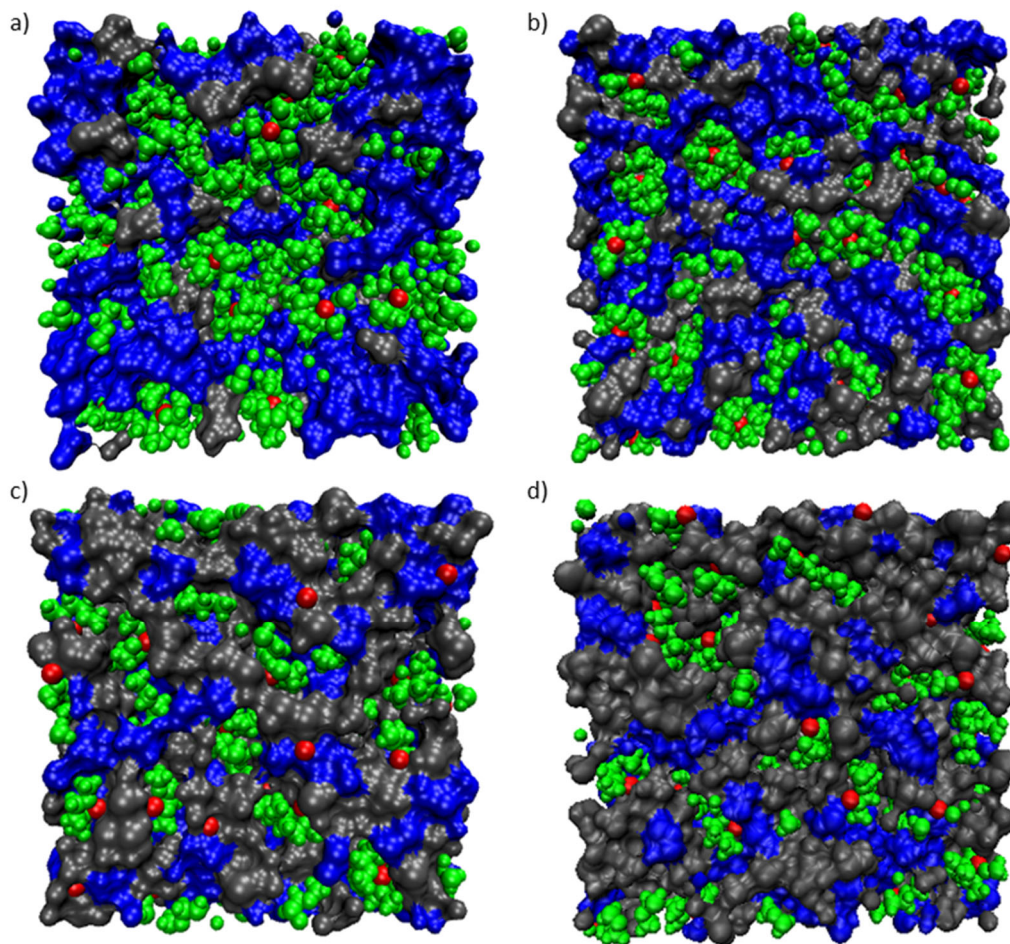


Fig. S9 Representation of the simulation boxes of the MD simulations for the conducting salt concentrations: a) 1 M, b) 3 M, c) 5 M, d) 7 M. Li⁺ cations are depicted in red, DME in green, and TFSI⁻ (gray) and DOL (blue) are shown as a surface to illustrate the domains they cover.

References

1. L. Suo, Y. S. Hu, H. Li, M. Armand and L. Chen, *Nat. Commun.*, 2013, **4**, 1481.